Experimental methods for Power Take-off (PTO) simulation of a Wave Energy Converter (WEC)

Nuno M. Ferreira[1], Marc D. Hadden[1]

[1] Martifer Energia S.A.
Dep. I&D
Porto Comercial Terminal Sul Apartado 39
3811-901, Aveiro, Portugal
nuno.ferreira@martifer.pt

Abstract

The objective of this paper is to describe one of the R&D stages of Martifer's WEC.

It is well known that one of the major difficulties in experimental wave testing is the reduced scale used and its implication on the typical methods utilized to determinate the possible energy conversion, as well as the methodology used to characterize the performance of a new WEC concept [1]-[2].

The WEC's concept and geometry were obtained using hydrodynamic analysis of several shapes and also in conformity with preliminary downscaled tests in regular wave states.

The main goal of these experimental tests were to simulate and observe the interactive behaviour of different configurations and methodologies for converting wave energy into usable energy, designated as its PTO system. In order to achieve this, several methods of growing complexity and accuracy were used to simulate the PTO system, from simple springs to more complicated friction based and compressed air type systems were used.

Described herein are the first set of tests, which include the limitations of the methods used, their results and the most relevant conclusions.

Keywords: experimental tests, methodology, Power take-off, PTO, Wave Energy Converter, Wave tank, WEC

Nomenclature

WEC = Wave Energy Converter
PTO = Power Take Off
H = Height of the wave (m)
T = Period of the wave (s)
s = second
m = metre

1 Introduction

In the development process of a WEC a wave test facility is important as it permits the determination and confirmation of important parameters.

One of the goals was to determinate the power generation that can be achieved by a WEC. However, as these experiences are scaled models, the resulting values of some parameters are more often than not very low, which in some cases creates difficulty in obtaining acceptable values [1] - [5].

The principle intention for this work was to complete preliminary studies to obtain a nearer to realistic value for power generation. To achieve this several methods were utilized to simulate the PTO.

These tests were performed with regular waves in a wave channel, built by Martifer Energia, the dimensions of which are: length 12m, width 2m, height 1,5m with a water depth of 0,8m. The test facility generates regular waves using a simple hinged paddle connected to an AC Motor and gear box, which in turn is controlled using a program developed in house. The test equipment was calibrated to produce regular wave periods between the ranges of 0,6 to 2,4 seconds and a maximum wave height of 0,3m. The equivalent real scale waves being between 6 and 14 seconds, and having a maximum height of 5,5m.

Table 1 shows the regular waves used for testing based on the wave climate along the Portuguese Coast [6].

		T (s)				
		6	**8**	**10**	**12**	**14**
H (m)	**0.5-1**				X	X
	1-1.5			X	X	X
	1.5-2				X	
	2-2.5	X	X	X	X	X
	2.5-3	X		X	X	X
	3-3.5		X	X	X	X
	3.5-4		X	X		
	4-4.5		X	X	X	
	4.5-5				X	
	5-5.5				X	

Table 1: Regular Waves Tested.

In order to perform these tests, a 1:40 scale concept model [7] – [9] was constructed using acrylic and PVC, as shown in figure 1.

The tests were completed using a model composed of two bodies which permits relative rotational oscillation about a single shaft.

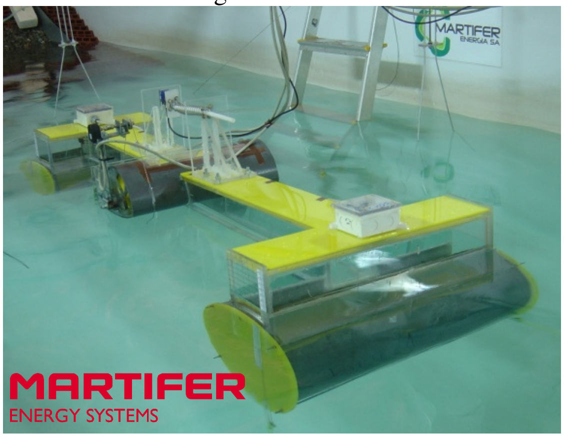

Figure 1: 1:40 Scale Model.

2 Test Methods

The general idea was to understand the influence of a PTO system on the model's behaviour by using several methods that could be compared to a fundamental hydraulic system, since it is what will be installed in the prototype.

However the principal reason for not using a hydraulic system is due to its scalability. As the tests were completed at a scale of 1:40, the use of a hydraulic cylinder could not be considered, due to its down scaling dimensional difficulties.

The PTO test methods described in Table 2, use standard equipment such as: springs, pneumatic cylinders, load cell and air pressure sensors.

Incorporated within the model a Full 360° Smart Position Sensor, model 601-1045 – Vishay Spectrol potentiometer was utilised to measure the angle between the two bodies (rotation) it also allowed the angular velocity between them to be determined. An AEP CTCA10K5 type load cell was also used to measure the force of the spring and the brake, and a PARKER P3HPA12AS2AD1A type pressure sensor and proportional valve were also installed to measure the pressure of the compressed air inside the cylinder.

The moment applied and the available power were determined using the force/pressure, angular motion and velocity.

The principal aim was to find a system that would solve the difficulties of the earlier methods tested, to achieve an optimum way in which to simulate PTO at a reduced scale, and so obtain a realistic value of the generation power available.

2.1 Spring method (S1)

In a common spring (Figure 2) the force has a linear increase in relation to its displacement, and no energy was dissipated, as it returned to its initial position after reaching its maximum value of force/displacement. To overcome this situation only the movement associated with the spring compression was considered.

Method	Description	Problem
Single spring (S1)	Spring in opposition unidirectional	Force increase with displacement, without pre charge,
Disc Brake (B1)	Bike brake, constant force along the movement	Difference between dynamic and static friction coefficients
Two springs (S2)	Spring in opposition bidirectional	Force increase with displacement
Pneumatic1 (P1)	Pneumatic cylinder	Pressure generated too low

Table 2: Test Methods.

A direct comparison between this method and a real scale hydraulic system cannot be made due to the inexistence of a pre-load in the system. To quantify the force applied by the spring a load cell was connect to one end. The displacement of the spring was measured by the relative angle between the two bodies through the potentiometer.

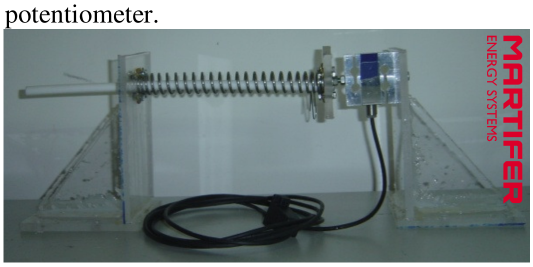

Figure 2: Spring Method.

2.2 Brake method (B1)

To try and overcome the difficulties of the pre-load and the force behaviour, an alternative method to simulate the PTO was to use a disc brake system type V-brake (Figure 3).

The disc brake system was connected to the shaft of the model. To estimate the force/moment applied on the PTO system the tension was measured using a load cell connected to the brake cable itself (which compresses the disc motion). By using the measured forces and the angular velocities the power could determinated. Note: That the angular velocity was calculated by using the displacement angle and the time taken for the displacement to occur.

It was initially thought that applying a small amount of pressure would result in low friction. However during the tests a problem was indentified which related to the difference between the static and the dynamic friction coefficients, resulting in a different opposition force (not constant).

Since the movement is oscillatory, it meant that the coefficient was changing constantly between the static (high value) and the dynamic friction (lower value), representing a change of the compressive force on the disc [10].

Only the static coefficient (static force) is being measured, which indicates that the dynamic force value is unknown (it is known to be lower than the static). This method represents a problem, which is that only the static moment applied to the shaft can be determined.

Figure 3: A brake bike model – SHIMANO®.

This method allowed the pre-loading of the brake, however, the associated value in relation to the motion is not very precise, even unknown.

2.3 Two spring method (S2)

Testing with two springs allowed for the possibility to pre-load both springs in accordance with the afore mentioned assembly manner (S1), since one worked in compression and the other in traction. The main intention with this method was to simulate the existence of a pre-load whilst trying to omit the power return. But the continual problem of the linear behaviour of the force versus displacement occurred.

2.4 Pneumatic method (P1)

The next step was to use a small pneumatic system, which consisted of a cylinder (1), a pressure sensor (2) and a proportional valve (3), see Figure 4. This method permitted pre-loading of the air pressure in the circuit, through the proportional valve.

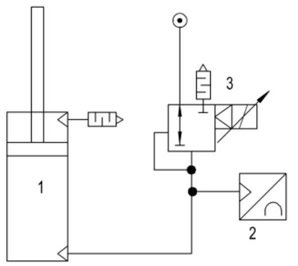

Figure 4: Pneumatic scheme.

The idea was to use the proportional valve to release the air when the pressure inside the cylinder chamber achieved its pre-set value, allowing the piston move. Only one chamber of the cylinder was used to compress the air, whilst several pre-set values were tested.

One problem that arose was related to the pressure generated in the cylinder chamber, which was sometimes lower than the minimum work pressure of the proportional valve. When this occurred the air was not released as the internal pressure could not reach the desired pre-set pressure. This was due to the fact that the necessary cylinder diameter was too small and could not be found on the market. This again is another scaling problem, the force to be measure was too low.

3 Results

The following graphs represent the qualitative behaviour of the different tested methods. These results correspond to the average relative height values obtained for each parameter (angle and moment) for the waves tested. All graphs are plotted in a linear scale, and the wave pattern used for each test method can be found in Table 1. The following data is a representation of the real scale prototype [1:1], although the recorded data was taken from a 1:40 scale model and upscaled using the Froude scaling laws.

3.1 Spring method (S1)

For the single spring method, several springs were tested with different spring coefficients.

Figure 5 simply shows the difference in the moment due to the increase in motion (angle) of two springs with different spring coefficient. From this graph it is possible to observe that 40º is the maximum angle measured for spring 1. This result confirms that spring 2 has a higher spring coefficient, as it has a higher moment value and lower angle than spring 1.

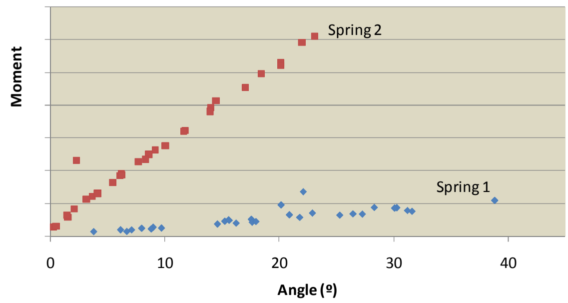

Figure 5: Moment versus angle for different springs.

In Figure 6 it is possible to observe the power/energy difference between the two springs, mainly in their resonance period. We can see that the power resonance period of the two springs (corresponding to the maximum value) is different: 10s for spring 2, and 12s for spring 1. This is possibly due to the difference of the spring coefficients between them, as observed in Figure 5.

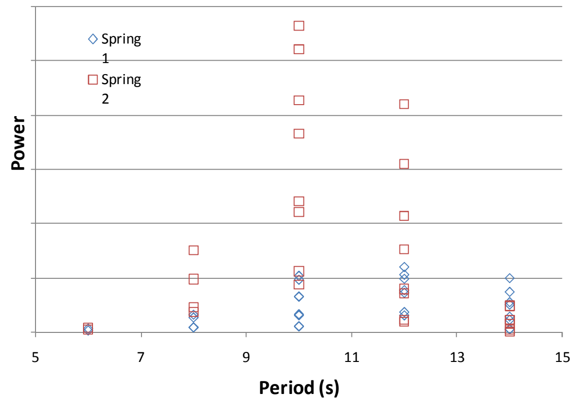

Figure 6: Power for the springs 1 and 2.

3.2 Brake method (B1)

From the results of the brake method we can observe the decreasing moment with respect to movement, unlike the spring situation (Figure 7). It can be observed that when the brake is activated a maximum angle of nearly 17º exists, compared to an angle of nearly 35º when left to move freely (without friction).

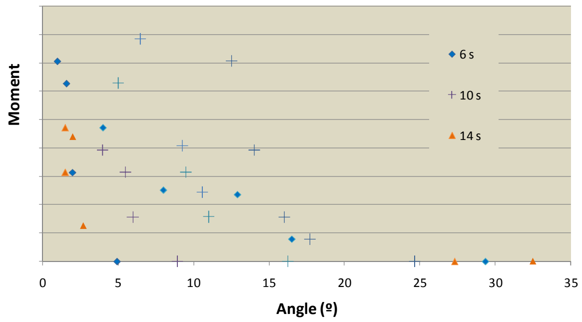

Figure 7: Moment versus angle for brake system.

In Figure 8 the maximum power reached was for a time period of 10s, confirming the value obtained in numeric simulation [7] - [9].

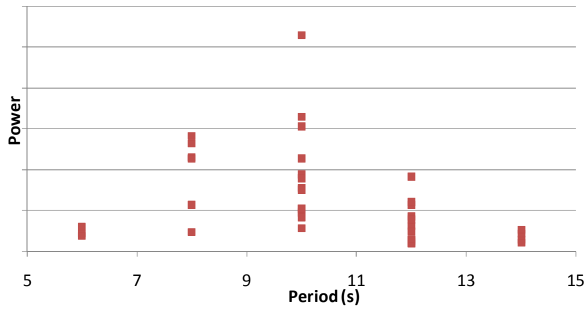

Figure 8: Power versus period for bike brake system.

3.3 Two spring method (S2)

For pre-loaded springs (S2) two main slopes can be seen on Figure 9, these are due to two different springs. On each spring two pre-loads were applied.

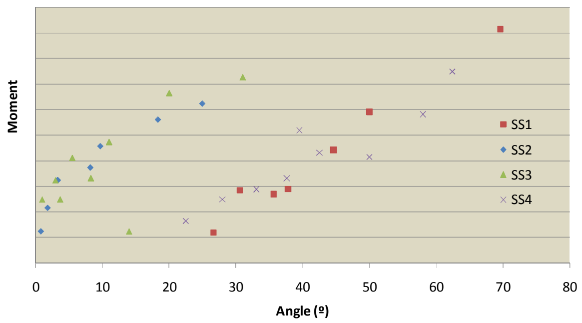

Figure 9: Moment versus angle for the pre-charge springs.

As expected a linear dependence for the springs was observed between the moment and the angle/displacement.

It can be shown that the origin of SS1 and SS4 are from the same spring (they simply have different pre-loads), since they have a similar development behaviour. SS2 and SS3 follow this same development behaviour but, correspond to another spring.

The relative pre-loads used in the tests are shown in the Table 3. It can be observed that SS1 has the highest relative value followed by SS2, SS3 and with SS4 having the lowest value.

Comparing the results shown in Figure 9 and with their subjected pre-load in Table 3, it can be seen that the slope development behaviour of the same spring is uniform and independent of the applied pre-load. The noted differences occurred for different springs, as was expected, based on previous results (Figure 5).

In this system a maximum angle of 70º was measured, which is a value far too high when compared with other values measured using other test methods. This situation could be due to the effect of the resonance period of the optimal spring coefficient.

Figure 10 shows the different behaviours between the pre-loads in terms of power.

Springs	Relative pre-loads
SS1	1.00
SS2	0.93
SS3	0.26
SS4	0.21

Table 3: Relative spring coefficients for the applied pre-loads in the spring system.

For this system the resonance period was found to continually be 10s, independent of spring type or pre.-loads. It can be proved from this figure that SS1 and SS4 continue to have higher relative power values, compared to SS2 and SS3. This is in accordance with the results obtained for the moment and angle (Figure 9).

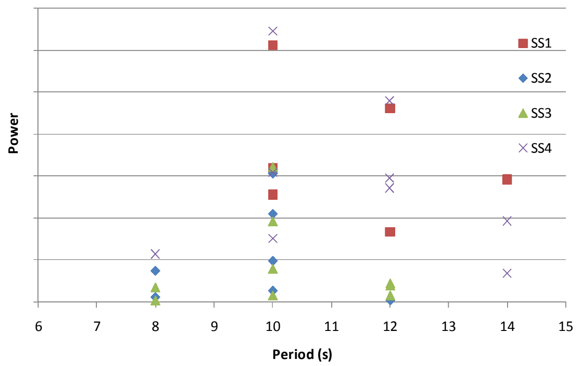

Figure 9: Power for the pre-loaded springs.

3.4 Pneumatic method (P1)

The results obtained from the pneumatic system where the changes in pre-load (denominated by F1 – F4) are shown in Figure 11. It is possible to see the difference between the pre-loads and their effects on the scatter curve behaviour. In this case a linear increase of the moment with respect to the angle can be observed.

However the slope is equal for all the pre-loads, as the only change is in the working pressure, since the cylinder diameter and the moment arm maintain constant for all the pre-loads.

The test denominated F3 shows a higher moment value, while test F1 shows a maximum angle near 50º.

Table 4 indicates the relative pre-loads between the situations tested. From the test results F3 shows a higher pre-load value with F2 followed by the F4 with the lowest F1. This order was same found in the moment figure 11.

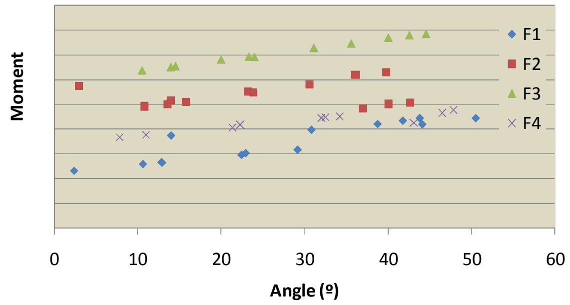

Figure 101: Moment versus angle for pneumatic cylinder.

The principal difference between this system and the other systems tested is the confirmed change of the resonance period, which in this case is 12s. This can be due to the change from spring to damping coefficients, which therefore explains the results of the resonance period change.

Test	Relative pre-load
F1	0.38
F2	0.76
F3	1.00
F4	0.58

Table 4: Relative damping coefficient for the pre-loaded pneumatic system.

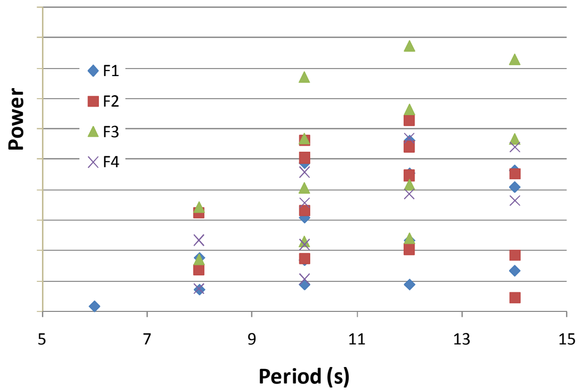

Figure 11: Power for pneumatic cylinder.

3.5 WEC behaviour

After testing all of the systems, a general increase of the power available from the PTO systems was registered (Figure 13) with wave heights of up to 3m. For higher waves a comparative decrease was observed between the obtained values for 3m and 4m, but from 4 to 5m an increase in these values was registered, as shown in Figure 13.

These results can be derived from the fact that the higher waves pass over the bow of the model, which in turn could imply a decrease in angle and moment value, resulting in lower power absorption as seen again in Figure 13.

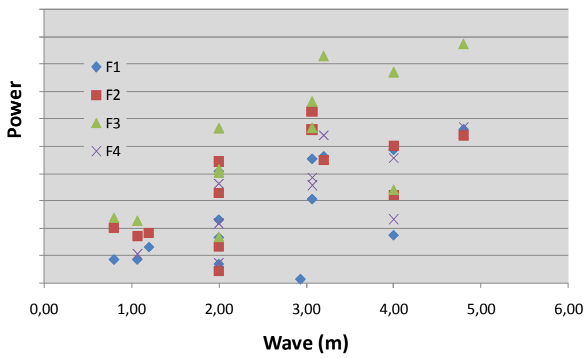

Figure 12: Power versus height wave for the pneumatic system.

The same behaviour for the angle with respect to the wave height can be seen, on tests where the model did not include a PTO system (free movement), as shown in the Figure 14.

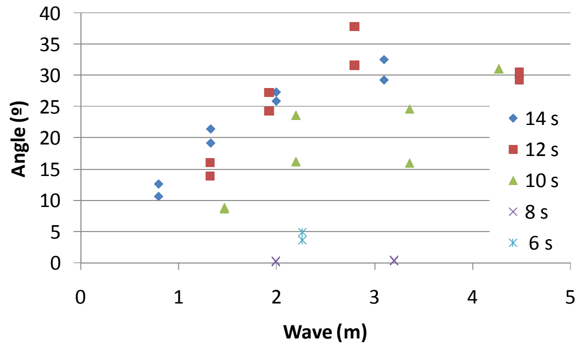

Figure 14: Angle versus height wave for without PTO.

Another interesting conclusion is that the angle has its resonance period at 12s, against the 10s expected when utilising the PTO system (Figure 15). This result can confirm the explanation given of the importance of the spring coefficient in the resonance period of all systems.

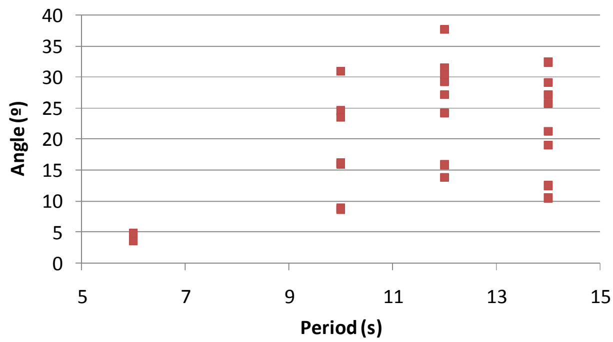

Figure 15: Angle versus wave period for without PTO.

4 Final Analysis and Conclusions

From the tests performed there were differences found in the behaviour between the various test methods. A comparison between the various methods can be seen using only the maximum power achieved in each of the individual test methods.

It is noted in Figure 16 that a significant difference between the methods in terms of magnitude of power with respect to wave height.

For the brake and pneumatic system it is possible to observe the decrease of the power in relation to wave heights from 3 to 4m as in Figure 16, in accordance to the results in Figure. 13.

The same result was observed for the angle when testing the model without PTO (free movement) (Figure 14).

The principle differences noted in the results were the changes in the resonance period for the pneumatic system (Figure 17). This change can be due to the importance of the damping coefficient against the spring coefficient.

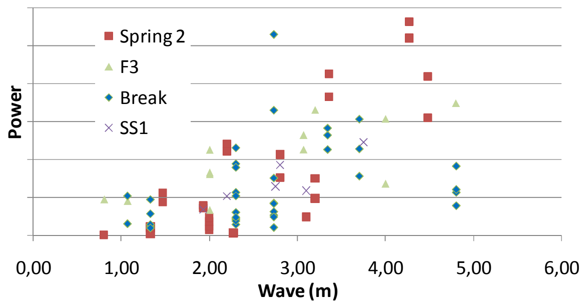

Figure 16: Power versus height wave for all systems.

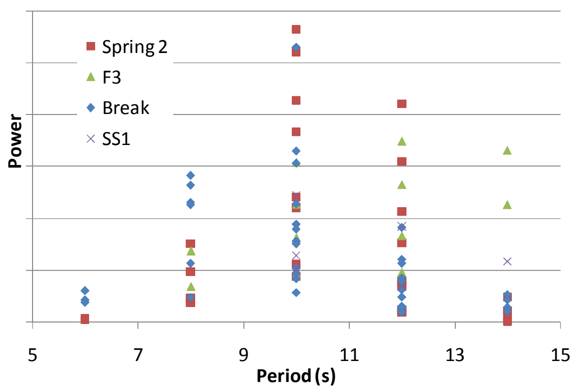

Figure 17: Power versus wave period for all systems.

The maximum angle measured on each system can be seen in Table 5.

Method	Maximum relative angle (º)
Without PTO	38
One spring (S1)	40
Brake (B1)	17
Two springs (S2)	70
Pneumatic1 (P1)	50

Table 5: Maximum relative angle measure in all the systems analysed.

Comparing all the systems tested, the brake system was confirmed to have the lowest angle. The reason for such was principally because a constant force is applied to the system. Unlike the other systems the force increases in relation to the angle/movement, this in turn explains the difference of the angles between the systems.

From the results it can be concluded that the spring coefficients are of great importance to the resonance period. The description in Table 2 for each method must be taken into account when experimentally simulating PTO systems.

5 References

[1]. Jens Peter Kofoed, Model testing of the wave energy converter Seawave Slot-Cone Generator, Aalborg University, April 2005

[2]. dti, Pelamis Wave Energy Converter, Verification of full-scale control using a 7th scale model, report related to the contract number: V / 06 / 00203 / 00 / 00, urn number: 05/653

[3]. A.J.N.A. Sarmento, Model-Test Optimization of an OWC Wave Power Plant, International Journal of Offshore and Polar Engineering, Vol. 3. No. I. March 1993 (ISSN 1053-5381)

[4]. Tony Lewis, Testing Procedures and Facilities for Ocean Energy Development, THIRD INTERNATIONAL SYMPOSIUM ON MARINE ENERGY, Bilbao, 2 April 2009

[5]. Ross Henderson, Design, simulation, and testing of a novel hydraulic power take-off system for the Pelamis wave energy converter, Renewable Energy 31 (2006) 271 – 283

[6]. Mariana Costa, Raquel Silva, João Vitorino, CONTRIBUIÇÃO PARA O ESTUDO DO CLIMA DE AGITAÇÃO MARÍTIMA NA COSTA PORTUGUESA, Instituto Hidrográfico, Rua das Trinas 49, 1249-093 Lisboa

[7]. Paulo Justino, José C. Amador, Tiago Morais, Marc Hadden, Nuno Ferreira, Frequency and time-domain models for a two-body wave power device that extracts energy from energy from sea waves by relative pitch motion, OMAE'08 - 27th International Conference on Offshore and Arctic Engineering, June 15-20, 2006, Estoril, Portugal.

[8]. N. Fonseca, J. Pessoa, R. Pascoal, T. Morais, R. Dias, Calculation of maximum pressure distributions for structural design of a floating wave energy converter, 2nd International Conference on Ocean Energy (ICOE 2008), 15th – 17th October 2008, Brest, France.

[9]. Fonseca, N., Pascoal, R., Marinho, J. and Morais, T., 2008, Analysis of wave drift forces on a floating wave energy converter, Proceedings 27th International Conference on Offshore Mechanics and Arctic Engineering (OMAE2007), paper OMAE2008-57941, Estoril, Portugal, 15-20 June 2008.

[10]. Bosch, Automotive Handbook 5th Edition, ISBN 0-7680-0669-4

Acknowledgements

We would like to acknowledge our co-workers Carlos Alves and João Pedro who helped in these experimental tests.